Hydrogel/electrospun fiber composites influence neural stem/progenitor cell fate

Anne Hsieh,[ab] Tasneem Zahir,[a] Yakov Lapitsky,†[a] Brian Amsden,[c] Wankei Wan[d] and Molly S. Shoichet*[abe]

Received 24th November 2009, Accepted 9th March 2010
First published as an Advance Article on the web 6th April 2010
DOI: 10.1039/b924349f

Cell replacement therapy with multi-potent neural stem/progenitor cells (NSPCs) into the injured spinal cord is limited by poor survival and host tissue integration. An injectable and biocompatible polymeric cell delivery system serves as a promising strategy to facilitate cell delivery, promote cell survival and direct cell behaviour. We developed and characterized the use of a physical hydrogel blend of hyaluronan (HA) and methylcellulose (MC) for NSPC delivery, and incorporated electrospun fibers of either collagen or poly(ε-caprolactone-*co*-D,L-lactide) (P(CL:DLLA)) to promote cell–matrix interactions and influence cell behaviour. The shear-thinning and thermally reversible HAMC had a zero-shear viscosity of 1.2 Pa s at 25 °C, formed a weak gel at 37 °C with a yield stress of 0.5 Pa, and swelled to 115% of its original volume after one day. HAMC was both cytocompatible and allowed NSPC differentiation *in vitro*, similar to what one would observe in media. Interestingly, cells cultured in HAMC remained homogeneously dispersed over the 7 d culture period, unlike those cultured in media controls where significant cell aggregation was observed. Inclusion of electrospun fibers in the HAMC hydrogel further influenced cell behaviour. Composite systems of collagen fibers in HAMC resulted in reduced survival/proliferation and differentiation relative to HAMC itself whereas composites of P(CL:DLLA) fibers in HAMC maintained cell survival/proliferation and enhanced neuronal and oligodendrocytic differentiation similar to HAMC. In this study, the importance of the cell delivery vehicle to NSPC survival and cell fate was demonstrated *in vitro* and is being tested in on-going studies *in vivo*.

1 Introduction

Traumatic spinal cord injury (SCI) results in cell death and cavity formation, disrupting signalling pathways of the central nervous system (CNS).[1] Patients often suffer lifetime sensory and motor deficits below the site of injury. Cell therapy is a promising strategy for tissue regeneration where, for example, neural stem/progenitor cells (NSPCs) have enhanced tissue repair and function after acute spinal cord injury.[2,3] NSPCs are multi-potent CNS cells capable of self-renewal and terminal differentiation into neurons, oligodendrocytes, and astrocytes. However, poor graft survival and integration are major factors limiting the efficacy of cell transplantation therapy. In previous studies, after bolus injection of NSPCs into the spinal cord, significant cell death was observed.[3,4] Notwithstanding the significant cell death after transplantation, selective ablation of engrafted cells in the spinal cord reversed the locomotor improvement previously observed.[5] The major challenges for stem cell transplantation studies are cell survival and directed cell differentiation.

By engineering the stem cell microenvironment using three-dimensional culture conditions, our goal was to enhance cell survival and differentiation. The choice of biomaterial, and its physical and chemical properties influence cell differentiation,[6] survival[7] and tissue integration.[8] Hydrogels are particularly compelling for cell delivery, having highly porous and hydrated structures that permit efficient diffusion of nutrients and oxygen, and metabolic waste products and CO_2. The hydrogel can be tuned either chemically with adhesive and differentiation factors or physically through crosslinking to yield a microenvironment that will influence cell proliferation and differentiation.[9,10] Hyaluronan (HA)-based hydrogels are compelling for cell delivery because HA is a naturally derived polysaccharide in the extracellular matrix and has some wound healing properties on its own.[11,12] While HA alone does not form a gel, a physical blend of HA and methylcellulose (MC) forms a gel due to the thermally reversible gelation properties of MC.[13] MC itself has been tested as a drug delivery/tissue engineering scaffold for treating traumatic brain injury.[14] Importantly, HAMC has been shown to have some therapeutic benefits when delivered to the intrathecal cavity after spinal cord injury and can be injected using a minimally invasive technique.[12,14–16]

Here we were interested in testing a HAMC formulation for cell delivery with and without the inclusion of electrospun fibers.

[a]*Department of Chemical Engineering and Applied Chemistry, University of Toronto, Toronto, Ontario, Canada M5S 3E5*
[b]*Institute for Biomaterials and Biomedical Engineering, University of Toronto, Toronto, Ontario, Canada M5S 3G9*
[c]*Department of Chemical Engineering, Queen's University, Kingston, Ontario, Canada K7L 3N6*
[d]*Department of Chemical & Biological Engineering, University of Western Ontario, London, Ontario, Canada N6A 3K7*
[e]*514 Donnelly Centre for Cellular and Biomolecular Research, 160 College Street, Toronto, Ontario, Canada M5S 3E1. E-mail: molly.shoichet@utoronto.ca; Fax: +1-416-978-4317; Tel: +1-416-978-1460*
† Current address: Department of Chemical and Environmental Engineering, University of Toledo, 2801 West Bancroft Street, Toledo, OH 43606, USA.

Our hypothesis was that the HAMC hydrogel would disperse the cells within the 3-D environment and that the electrospun fibers would provide substrates for cell adhesion and thereby influence the differentiation profile of the stem/progenitor cells cultured within the fiber/hydrogel composite. We chose to compare the influence of two electrospun fibers dispersed within HAMC—naturally derived collagen *vs.* synthetic poly(ε-caprolactone-*co*-D,L-lactide)—*vs.* HAMC alone. HAMC was first evaluated in terms of time to gelation, rheology and swelling to determine whether it met our design criteria for fast gelation, facile injection, and minimal swelling so as not to compress the tissue after injection. The *in vitro* compatibility of NSPCs dispersed in HAMC was evaluated by measuring the number of live cells and their metabolic activity in three media conditions, compared to media alone controls. The electrospun fibers were chosen to represent two ends of the spectrum in terms of composition and diameter: naturally derived collagen *vs.* synthetic P(CL:DLLA), and nanometre to micrometre diameter fibers. Both types of fibers were sonicated to allow their dispersion in HAMC. Then the differentiation profile of the NSPCs in HAMC (with and without the fibers) was studied using immunocytochemistry and quantitative RT-PCR. In these series of studies, our goal was to evaluate the cellular response *in vitro* to the different culture conditions with a view of applying this knowledge to an *in vivo* system.

2 Materials and methods

2.1 Preparation of HAMC hydrogel

HA and MC were sterile-filtered as dilute aqueous solutions in deionized water through 0.22 μm vacuum filters (Nalgene, Rochester, NY, USA) and lyophilized prior to use.[12] HAMC 0.5/0.5 was prepared with 0.5 wt% HA (M_w 1 500 000, Novamatrix, Norway) and 0.5 wt% MC (M_w 310 000, ShinEtsu Metolose SM-4000, Japan) dissolved in one of three cell culture media: (1) basic media: neurobasal media (Gibco-Invitrogen, Burlington, ON, Canada) supplemented with B27 neural supplement (Invitrogen), 2 mM L-glutamine (Sigma-Aldrich, Oakville, ON, Canada) and 100 μg mL^{-1} penicillin–streptomycin (PenStrep, Sigma-Aldrich); (2) differentiation media: basic media supplemented with 1% fetal bovine serum (FBS) (Invitrogen); (3) proliferation media: basic media supplemented with 20 ng mL^{-1} epidermal growth factor (recombinant human EGF, Invitrogen), 20 ng mL^{-1} basic fibroblast growth factor (recombinant human bFGF, Invitrogen) and 2 μg mL^{-1} heparin (Sigma-Aldrich).

2.2 Preparation of electrospun fibers

Electrospun fibers of genipin crosslinked collagen and poly(ε-caprolactone-*co*-D,L-lactide) (P(CL:DLLA), 20 : 80 mol : mol CL : DLLA) fibers were prepared as previously described,[17–19] with average diameters of 265 ± 83 nm (and a range of 100 to 500 nm) and 2.1 ± 0.1 μm (and a range of 0.3 to 8.5 μm), respectively. The collagen fibers were disinfected by immersion in 70% ethanol for one day whereas the P(CL:DLLA) fibers were sterilized by gamma irradiation (Co-60, 2.5 mRad). The fibers were washed (3 times, 2 h each time) in basic media and then sonicated (Sonics Vibra Cell CV18 tip sonicator) twice consecutively for 30 s at 20 kHz, 25% amplitude. The resulting fiber fragments were easily incorporated into the HAMC, which was still injectable through the fine 30 gauge needle. For each study, there were 5 mg mL^{-1} of electrospun fibers dispersed in cell culture medium.

2.3 Mechanical testing and gelation time

2.3.1 Rheological evaluation. The rheological properties of HAMC were characterized by a stress-controlled steady state experiment at 25 °C and 37 °C using an AR2000 rheometer (TA Instruments, New Castle, DE, USA) equipped with a 60 mm, 0.5° cone. To allow thermal equilibration to occur, all samples were conditioned for 20 min prior to shear. Measurements were then performed at shear stresses ranging from 0.01 to 80 Pa at both 25 °C and 37 °C.

2.3.2 Inverted tube test. 300 μL HAMC made in basic medium were injected into the bottom of a 1.7 mL microcentrifuge tube (Fisher Scientific, Ottawa, ON, CA) and incubated at 37 °C. At 5, 10, 12, 14, 16, 18, and 20 min intervals, tubes were inverted to observe if the gel flowed. The time at which the gel did not flow was recorded as the gelation time.

2.4 *In vitro* swelling test

100 μL of 0.5/0.5 w/w% HAMC made in media were added to a 1.7 mL Eppendorf tube that was equilibrated at 37 °C. On the top of the gel, 900 μL of 37 °C artificial cerebrospinal fluid (aCSF), 0.5 mM NaCl, 5 mM KCl, 1.3 mM $MgCl_2$, 0.1 mM $CaCl_2$, 26 mM $NaHCO_3$, and 10 mM D-glucose, pH 7.4, were added. After set-up, half of the media was removed from the tubes every 24 h and exchanged with fresh incubation media. To study the trend transiently, samples were collected at each time point. At 0, 8 h, 1, 3, 6, and 9 days of incubation, all the media were removed and the weight of the wet gel was recorded ($n = 4$). Swelling was quantified as a function of time.

$$\%\ \text{Swelling} = \frac{\text{wet gel weight } (t)}{\text{wet gel weight } (t = 0)} \times 100\%$$

2.5 Neural stem/progenitor cell isolation and culture

Neural stem/progenitor cells were isolated from the subependyma of the lateral ventricles of adult female Wistar rat forebrains, as described previously.[20] Briefly, subependymal tissue was harvested from 8–12 week old rats and dissociated with papain (Papain Dissociation System, Worthington Biochemical Corporation, Lakewood, NJ, USA). The resultant cell suspension was centrifuged and the pelleted cells were subjected to a discontinuous density gradient to remove cell debris. Dissociated cells were re-suspended in proliferation media. The cells were incubated at 37 °C in a humidified incubator with 5% CO_2. Neurospheres appeared in 2–3 weeks, after which cells were passaged every week. All cell studies used neurospheres at passages 4 and 5.

2.6 Cell seeding

Neurospheres were centrifuged and washed once in basic media. A small sample of neurospheres was triturated into single cells

and counted with a hemacytometer using trypan blue (Sigma-Aldrich) exclusion to determine the starting live cell population. Neurospheres were cultured for 4 d in the *in vitro* biocompatibility study because, after 4 d, there was significant aggregation of neurospheres in the proliferation media, which made the results difficult to interpret. Dissociated single cells were cultured for 7 d for the differentiation profile studies. 2×10^4 NSPCs were dispersed in 100 μL of either: media alone, HAMC, electrospun collagen fiber/HAMC or electrospun P(CL:DLLA) fiber/HAMC and then loaded into 1 mL syringes and injected through 30 G, 1″ needle into black clear-bottom 96 well plates (Greiner, Germany). 200 μL of media were added on day 3 to supply nutrients in the 7 d cultures. Cells were imaged on an inverted microscope (Axiovert S100, Zeiss) equipped with a camera (Cool SNAP HQ, Photometrics) on days 2 and 7.

2.7 NSPC viability/proliferation study

2.7.1 Quant-iT™ PicoGreen® dsDNA Kits. NSPCs were collected from cell culture wells into a 1.7 mL Eppendorf tube, spun down at 3000 rpm for 5 min and washed once in sterile PBS. NSPCs were lysed through a freeze–thaw cycle in 1× Tris–EDTA buffer and 0.2% Triton X-100 (Sigma-Aldrich). Total double stranded DNA was measured by fluorescence (Molecular Devices) by the reaction of DNA with PicoGreen (PicoGreen dsDNA Quantitation Kit, Invitrogen). An internal standard curve was prepared and used to convert the concentration of dsDNA to total number of cells. The data were expressed as fold growth relative to number of NSPCs seeded at time zero.

2.7.2 CellTiter-Glo Luminescent Cell Viability Assay. CellTiter-Glo® Luminescent Cell Viability Assay (Promega, Madison, WI, USA) quantifies the cytoplasmic Adenosine Triphosphate (ATP) present, an indicator of metabolically active cells. Addition of the CellTiter-Glo® reagent results in cell lysis and generates a luminescent signal proportional to the total amount of ATP present in the viable cells. 100 μL of CellTiter-Glo® reagent were added to the culture well and placed on a rotary shaker plate for 10 min in the dark. Luminescence was recorded immediately after using a SpectraMax Gemini EM microtiter plate reader (Molecular Devices Corporation, Sunnyvale, CA, USA). The mean background luminescent signals from the media and cell-free HAMC controls were subtracted from the luminescence signals from the NSPCs in media and HAMC samples, respectively.

2.7.3 LIVE/DEAD® Viability/Cytotoxicity Assay. Cell viability was quantitatively assessed with a Live/Dead kit (Molecular Probes, Eugene, OR). To prepare the cells, the cells were collected in a 1.7 mL Eppendorf tube, spun down at 3000 rpm for 5 min and then the supernatant removed. The cell pellet was then re-suspended in sterile PBS with 2 μM calcein-AM (a live cell fluorescent dye, 485/530 nm) or 10 μM ethidium homodimer (a dead cell fluorescent dye, 530/645 nm).

2.8 Electrospun fiber cytotoxicity study

Electrospun fibers of genipin crosslinked collagen and P(CL:DLLA) were sonicated as described in Section 2.2 to allow injection through the 30 gauge needle, placed in culture inserts (0.4 μm, BD Biosciences, Franklin Lakes, NJ, USA) and immersed in neural basal medium (NBM), incubated at 37 °C and 5% CO_2 for 7 days. The conditioned media were then used to culture NSPCs at a density of 2×10^4 single cells per 100 μL for 7 days. Cell viability was examined using PicoGreen and CellTiter-Glo® assays, as described above.

2.9 NSPC immunohistochemistry

2.9.1 Cryostat sectioning. Single cell cultures of 2×10^4 single cells per 100 μL of HAMC were grown for 7 d in the differentiation medium. Cryomatrix (Thermo Scientific, Pittsburgh, USA) was added to the well and placed at room temperature for 5 min, then snap frozen. 20 μm sections were cut using a cryotome (Leica CM3050, Bensheim, Germany), and mounted on glass slides.

2.9.2 Immunostaining. The following primary antibodies were used for immunohistochemistry (IHC) : monoclonal mouse anti-βIII-tubulin (1 : 1000, Abcam, Cambridge, MA, USA) for neurons; RIP monoclonal anti-2′,3′-cyclic nucleotide 3′-phosphodiesterase (CNPase) (1 : 5, Developmental Studies Hybridoma Bank, Iowa City, IA, USA) for oligodendrocytes; monoclonal mouse anti-glial fibrillary acidic protein (GFAP, 1 : 100, Cell Sciences, Canton, MA, USA) for astrocytes; and monoclonal mouse anti-nestin (1 : 500, BD Biosciences, San Jose, CA, USA) for progenitor cells. After 7 days in culture, cells were fixed in 4% paraformaldehyde (Sigma-Aldrich) in PBS for 20 min at room temperature and then washed with PBS 3 times. Cell membranes were permeabilized with 0.1% Triton X-100 in PBS for 10 min, washed 3 times, then blocked with a solution of 10% FBS in PBS at room temperature for 1 h. Next, each primary antibody solution was added for 2.5 h at 25 °C. After washing with PBS 3 times, samples were exposed to goat anti-mouse IgG Alexa-Fluor 546 (1 : 400, Invitrogen) for 2 h at room temperature and then washed with PBS buffer 3 times. Finally, cell nuclei were counterstained with 10 μM Hoechst 33342 (Invitrogen) for 7 min, washed with PBS buffer and mounted/cover slipped using ProLong Gold anti-fade reagent (Invitrogen). Fluorescent signals were detected and imaged *via* confocal laser scanning microscopy (Olympus BX61, Ontario, Canada) equipped with a camera (Olympus DP70).

2.10 Total RNA isolation and real-time RT-PCR

To monitor the expression level of differentiation gene markers using qRT-PCR, total RNA from the cells was prepared. Cells were collected at day 7 into 2 mL screw-cap microvials with 1.0 mm Zirconia Beads (BioSpec Products, Bartlesville, OK, USA), and homogenized using the mini-beadbeater-16 (BioSpec Products) for 3 min. Total RNA was isolated using the acid guanidinium thiocyanate–phenol–chloroform extraction method, with 1 mL Trizol reagent (Invitrogen) and 0.2 M potassium acetate to remove the polysaccharide (HAMC) from the sample before adding chloroform for RNA extraction.

After RNA isolation, DNase I treatment was performed followed by the measurement of total RNA concentration and purity (NanoDrop ND-1000). For the reverse transcription (RT) reaction, 15.7 μL of RNA (at 5 ng total RNA per μL) were

incubated with oligo(dT) primers and random hexamers at 65 °C for 5 min. After the sample has cooled from the 65 °C in the previous step to room temperature, the RNA-oligo(dT)/hexamer mix, buffer, dNTPs, RNase inhibitor, Stratagene AffinityScript RT enzyme (La Jolla, CA, USA) were then added to the sample and heated to 42 °C for 60 min. The reaction was terminated by heating at 70 °C for 15 min. Quantitative reverse transcriptase-polymerase chain reaction (qRT-PCR) amplification was performed with a Roche LightCycler® 480 (Laval, Quebec, Canada) using SYBR Green I (Invitrogen) detection chemistry. The 5′ to 3′ sequences for the forward primers and reverse primers were previously designed in our lab from rat mRNA sequences from the National Center for Biotechnology Information (NCBI). For qRT-PCR analysis of each sample, the following were prepared in a 11 μL reaction buffer: 1 μL of DNA sample, buffer, 3–4 mM $MgCl_2$, 0.2 mM DNTPs, 200–400 nM of each forward and reverse primer, 0.5× SYBR Green I, 1× ROX reference dye (Sigma-Aldrich), and 0.055 U HotStarTaq (Qiagen, Valencia, CA, USA). Quantitative RT-PCR amplification was achieved with a 15 min activation step at 95 °C, followed by 50 cycles of 15 s at 94 °C, 30 s at 60 °C, 60 s at 72 °C and a fluorescence measurement (excitation/emission—494/521 nm). All qRT-PCR reactions were performed in triplicate. A standard curve (cycle threshold value *versus* relative template concentration) was prepared for each target gene and for the endogenous reference (HPRT). Gene expression for each target gene was compared across experimental groups, and the relative fold change was calculated by normalizing against the endogenous reference genes using Pfaffl's efficiency corrected calculation model for multiple reference genes. The primer sets used for βIII-tubulin, 2′,3′-cyclic nucleotide 3′-phosphodiesterase (CNPase), glial fibrillary acidic protein (GFAP), nestin, and hypoxanthine phosphoribosyltransferase 1 (HPRT) were as previously published by Leipzig and Shiochet.[21]

2.11 Statistical analysis

All statistical analyses were performed using JMP IN 7.1 (SAS Institute, Cary, NC, USA). Differences among groups were assessed by ANOVA with Tukey's *post hoc* analysis to identify statistical differences among three or more treatments. All errors are given as standard deviation.

3 Results

3.1 HAMC characterization

The 0.5/0.5 w/w% HAMC hydrogel was characterized by time to gelation, rheology and swelling. By the inverted tube test, HAMC gels after 18 min at 37 °C. The shear stress (τ) *vs.* shear rate (γ) data in the limit of low shear rate for HAMC at both 25 and 37 °C are illustrated in Fig. 1a. At 25 °C, HAMC displays nearly Newtonian behaviour—that is a linear shear stress *vs.* shear rate relationship without a yield stress, where $\tau = \eta \times \gamma$ reflecting the nearly constant viscosity in the low-shear portion of the flow curve (Fig. 1b). At 37 °C, however, a yield stress of 0.5 Pa is observed. Thus, the blend exhibits nearly perfect Bingham

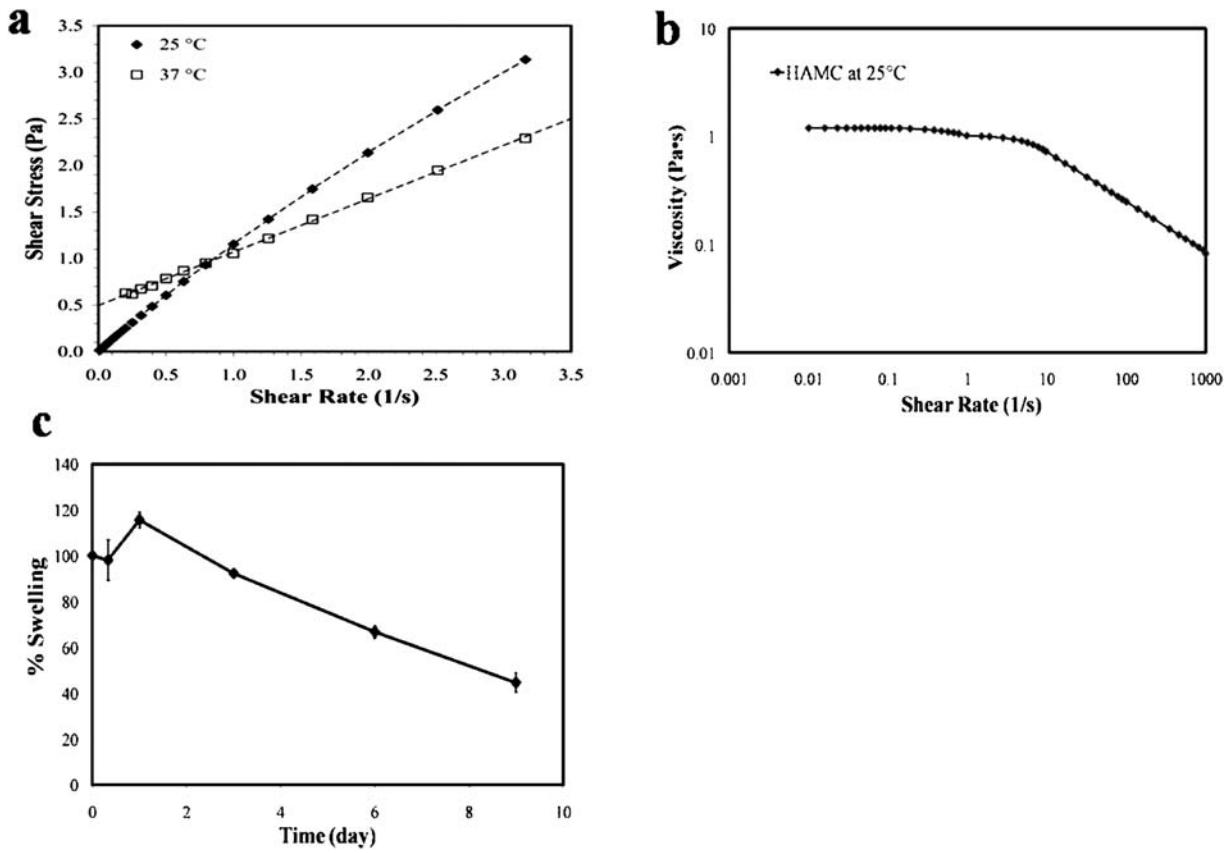

Fig. 1 HAMC was characterized by: (a) shear stress *vs.* shear rate, demonstrating a yield stress at 37 °C; (b) viscosity *vs.* shear rate, demonstrating shear-thinning; and (c) swelling.

plastic behaviour, according to $\tau = \mu_p \times \gamma + \tau_y$ where μ_p is the plastic viscosity of approximately 0.6 Pa s and a yield stress of 0.5 Pa, which corresponds to the formation of a very weak gel.

To gain greater insight into the injectability of HAMC at the 0.5/0.5 w/w% composition, its viscosity at room temperature was characterized over a broader range of shear rates. At room temperature (25 °C), HAMC is a moderately viscous solution with shear thinning properties (Fig. 1b). This rheological signature is characteristic for polymeric solutions[22] where the viscosity, η, remains nearly constant ($\eta = 1.2$ Pa s) at low shear rates and decreases with a power law relationship at high shear rates, and in this case, with a scaling exponent of ~0.5.

Since HAMC is designed to be injected into a tissue cavity, the degree of gel swelling was investigated to ensure minimal tissue damage such as compression of the soft tissue at the injured site. The swelling of HAMC reached a maximum swollen volume of approximately 115 ± 14.6% by 1 day and gradually decreased to 50 ± 4.2% by day 9 (Fig. 1c).

3.2 NSPCs cultured in HAMC *vs.* media: cell distribution

NSPCs cultured in media were compared to those cultured in HAMC in terms of cell distribution over time. As shown in bright-field images (Fig. 2), NSPC neurospheres cultured in proliferation media of EGF/FGF2/heparin alone aggregated (Fig. 2a) whereas those cultured in differentiation media in HAMC remained dispersed in the gel (Fig. 2b). The aggregated neurospheres cultured in media had darkened necrotic cores, likely due to their increased size, unlike those cultured in HAMC. In differentiation media containing 1% FBS, NSPC neurospheres displayed irregular non-circular cell morphologies and no process formation when cultured in media *vs.* HAMC. Interestingly, there was little evidence of differentiation after 48 h of NSPCs cultured in differentiation media alone, where the cell body remained spherical (Fig. 2c). In contrast, NSPCs cultured in differentiation media in HAMC extended processes and formed networks (Fig. 2d).

3.3 NSPC viability in HAMC *vs.* media controls

The number of NSPCs cultured in HAMC was compared to those in media after 4 days of culture using the dsDNA content measured by the PicoGreen assay as a proxy for cell number. Importantly, cells cultured in HAMC were injected *via* a 30 gauge needle into the culture well, thereby simulating the *in vivo* injection procedure. The day 4 data were normalized to day 0 to account for any variability in the number of NSPCs seeded. The number of NSPCs cultured in media was comparable to those dispersed in HAMC (Fig. 3a). In basic culture conditions, there were more live cells in HAMC relative to the media control. While no significant difference was observed among cells grown in media *vs.* HAMC for the other media conditions, NSPCs grew more rapidly when cultured in the presence of mitogens (EGF/FGF2) than the basal and differentiation media conditions.

To assess the metabolic activity of NSPCs in different culture conditions, total cellular plasma ATP was measured using the luminescence assay (Fig. 3b). No difference was found between cells cultured in basal or differentiation media conditions; however, cells cultured in the EGF/FGF2 proliferation media had higher ATP content per live cell. Interestingly, cells cultured in this proliferation media in HAMC had a lower luminescent signal, and thus less ATP/live cell, than cells cultured in the proliferation media alone.

To gain a thorough understanding of how the culture environment affected cell viability, the percentage of live cells, by calcein AM staining, and the percentage of dead cells, by ethidium bromide homodimer, were measured (Fig. 3c and d). The percentage of live cells was similar for NSPCs cultured in neurobasal or differentiation media with and without HAMC. However, the percentage of live cells was lower in the proliferation media, whether cultured in HAMC or media, relative to the

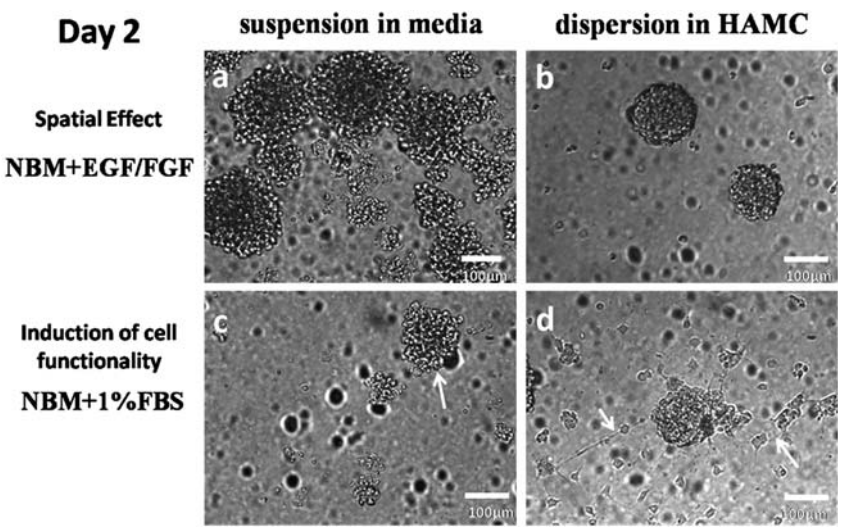

Fig. 2 Bright-field microscopic images of NSPC neurosphere cultures at day 2: (a) cells cultured in proliferation media aggregated whereas those cultured in (b) proliferation media in HAMC remained dispersed throughout the gel. (c) NSPC neurospheres cultured in differentiation media remained spherical whereas (d) NSPC neurospheres cultured in differentiation media in HAMC extended processes and formed networks with other neurospheres. Arrows highlight processes and morphological changes of NSPCs in (d).

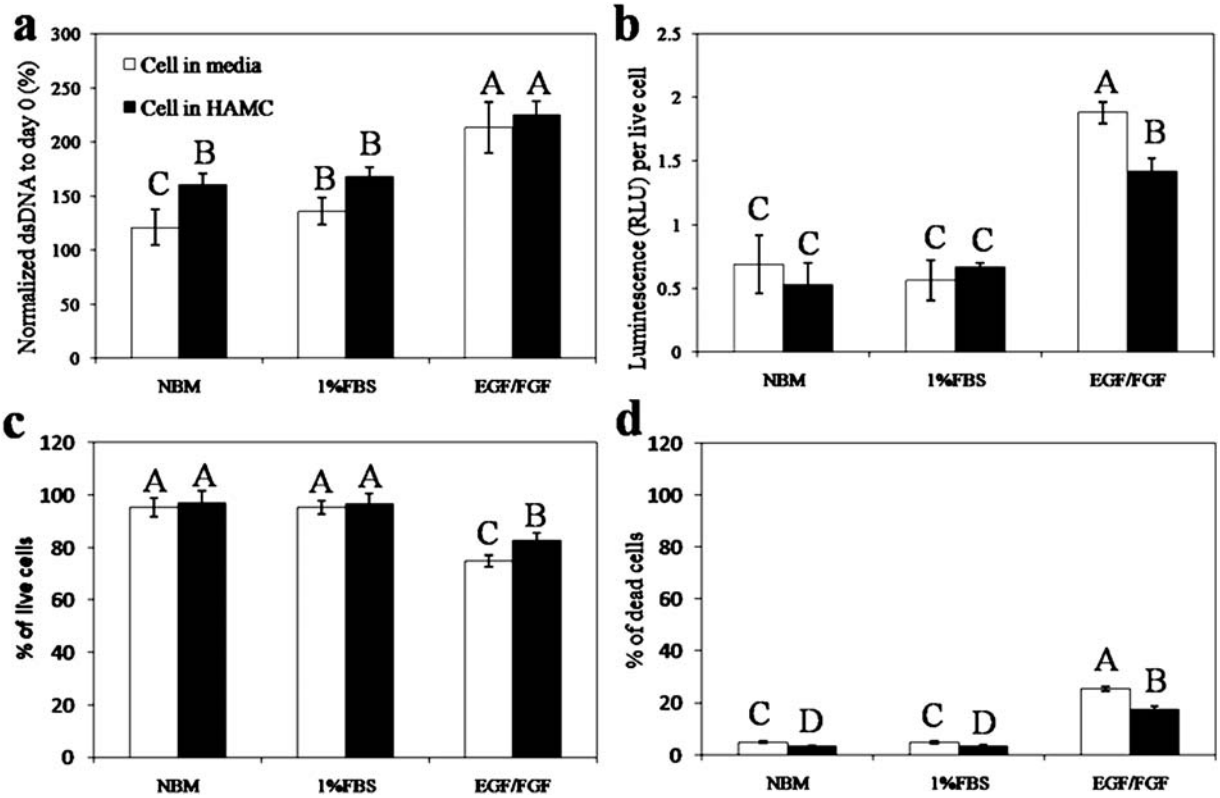

Fig. 3 NSPC neurospheres cultured in different media alone *vs.* different media in HAMC after 4 days. (a) The PicoGreen assay for dsDNA shows a greater number of cells in the EGF/FGF2 proliferation media and comparable numbers for cells cultured in media or HAMC; (b) CellTiter Glo luminescence assay for ATP shows greater ATP content per cell for cells cultured in the proliferation media than in basal and differentiation media conditions. Within the same media condition, cellular metabolic activity in HAMC was comparable to media controls in basal and differentiation conditions; however, the ATP content per live cell was higher in the proliferation media control *vs.* HAMC. (c) By calcein AM, the percentage of live cells was similar for basal and 1% FBS differentiation media, yet lower in the proliferation media, where there was a lower percentage of live cells in media *vs.* HAMC. (d) By ethidium homodimer, the percentage of dead cells was lower in HAMC than media controls for all media conditions. Of the media conditions, the percentage of dead cells was greater in the proliferation media (mean ± standard deviation are shown for $n = 3$; different letters indicate significant differences between the data at $p < 0.05$).

basal and differentiation media. Interestingly, there were more live cells in HAMC than media controls cultured in the EGF/FGF2 proliferation medium. Thus, while the PicoGreen data for dsDNA (Fig. 3a) showed greater numbers of cells in the proliferation media, the percentage of live cells was lower in the proliferation media than the other media conditions and HAMC, which is consistent with the bright-field microscopic images of Fig. 2. There was no difference in the percentage of dead cells in the basal or differentiation media for cells cultured in media or HAMC; however, there was a higher percentage of dead cells cultured in the proliferation media relative to the basal and differentiation media conditions. Moreover, there were more dead cells cultured in proliferation media than proliferation media in HAMC. These data are consistent with the live cell data and reflect the necrotic cores visualized in the neurospheres cultured in proliferation media alone *vs.* those in HAMC.

3.4 NSPC differentiation capacity in HAMC

NSPCs have been previously shown to differentiate to neurons, oligodendrocytes and astrocytes when cultured in 1% FBS

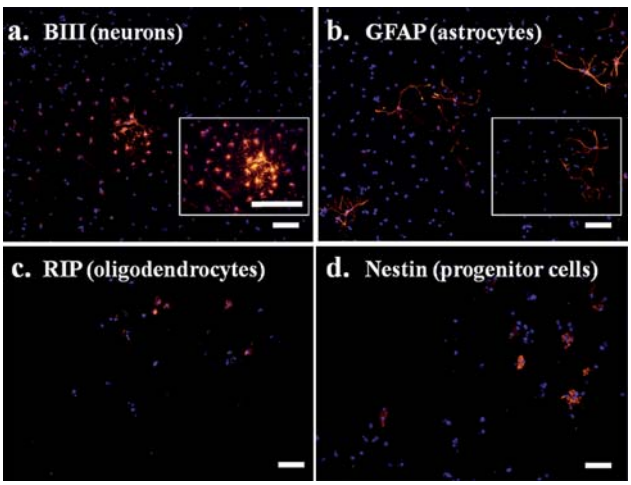

Fig. 4 NSPCs cultured in HAMC in 1% FBS media for 7 d differentiated to: (a) βIII-tubulin-positive neurons; (b) GFAP-positive astrocytes; (c) RIP-positive oligodendrocytes; and (d) nestin-positive progenitor cells. Cell nuclei were stained with Hoechst shown in blue. Scale bar is 200 μm.

supplemented media.[23] To ensure that NSPCs maintain this differentiation capacity when cultured in HAMC, the cells were characterized by immunohistochemistry after 7 d of culture. Fluorescent microscopy showed cells stained positive for: βIII-tubulin for neurons (Fig. 4a); GFAP for astrocytes (Fig. 4b); RIP for oligodendrocytes (Fig. 4c); and nestin for neural precursor cells (Fig. 4d). These data demonstrate that HAMC impacts neither the differentiation capacity of NSPCs to neurons, astrocytes and oligodendrocytes, nor the presence of the precursor population.

3.5 NSPC viability in electrospun fiber/HAMC composites

Prior to testing NSPCs in the composite system, the P(CL:DLLA) and collagen electrospun fibers were sonicated to allow injection through the 30 gauge needle and then

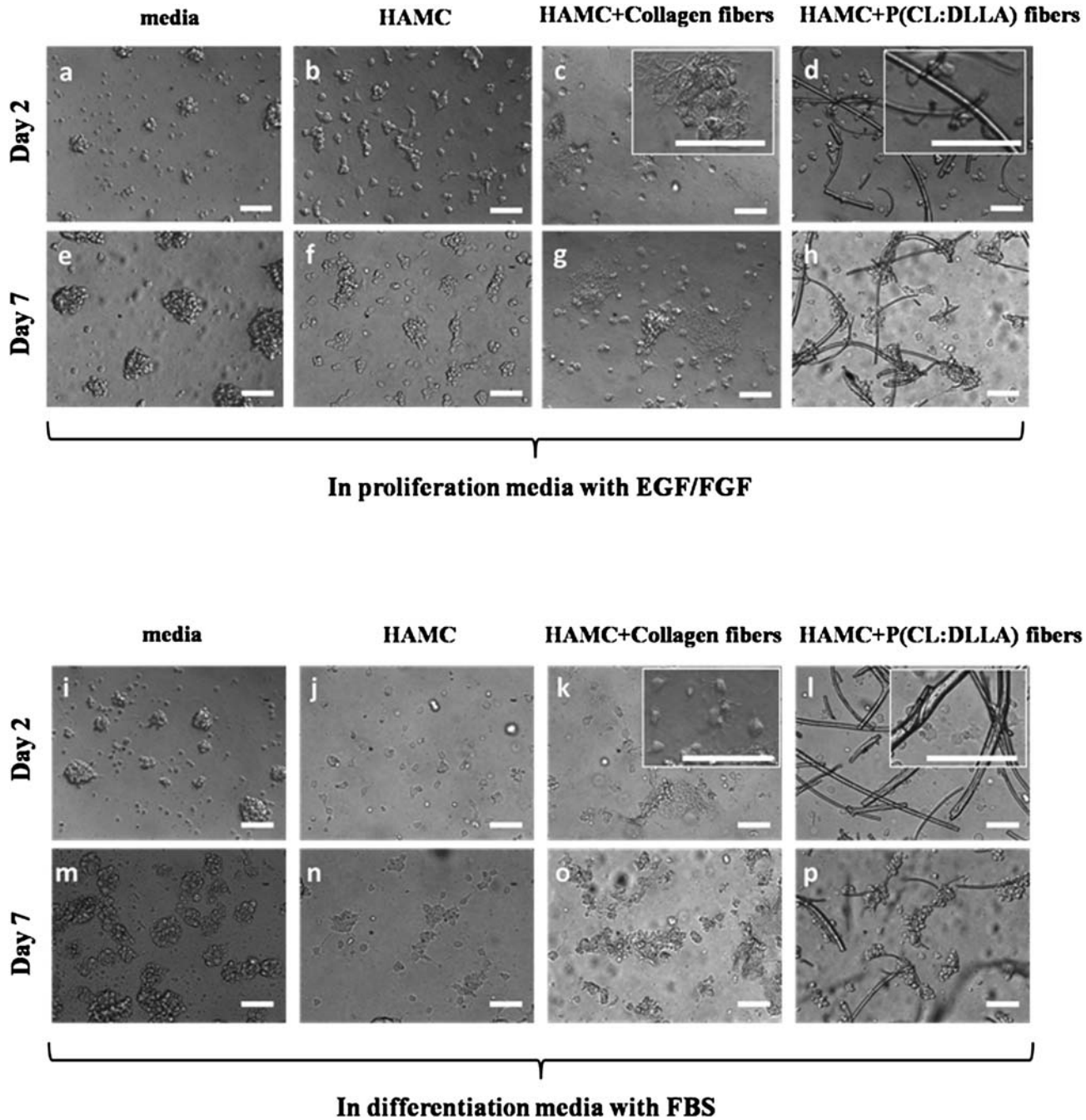

Fig. 5 Bright-field microscopy of NSPCs seeded as single cells and cultured in proliferation media (EGF/FGF2) for 2 days (a–d) and 7 days (e–h) in: (a and e) EGF/FGF2 media; (b and f) HAMC; (c and g) collagen/HAMC composite; and (d and h) P(CL:DLLA)/HAMC composite. The identical experiment was repeated for NSPCs cultured in FBS differentiation media for 2 days (i–l) and 7 days (m–p) in: (i and m) FBS media; (j and n) HAMC; (k and o) collagen/HAMC composite; and (l and p) P(CL:DLLA)/HAMC composite. Scale bar is 100 μm.

independently screened for cytotoxicity. The fibers were separately immersed for 7 d in the basic media that was then used to culture NSPCs for 4 d. Cell viability (using the PicoGreen assay for dsDNA) and metabolic activity per live cell (using the luminescence assay) were measured, and no differences were observed when compared to the media controls (data not shown). Nothing eluted from the fibers that was cytotoxic to NSPCs.

Electrospun fibers were sonicated into small fragments and then dispersed in HAMC with NSPCs prior to injection through a 30 G needle used for cell delivery. As shown in Fig. 5, NSPCs were distributed throughout the HAMC and fiber/HAMC composite gels at both day 2 and day 7 whether cultured in proliferation (EGF/FGF2) or differentiation (FBS) media. For cells cultured in the proliferation media, at day 2, there was little difference between media controls (Fig. 5a) and HAMC systems (Fig. 5b–d); however, the NSPCs appeared to be in close contact with the electrospun collagen fibers (Fig. 5c, inset) and to extend their processes toward and adhere to the P(CL:DLLA) electrospun fibers (Fig. 5d, inset). At day 7, cells suspended in media formed larger clusters due to cell aggregation and proliferation (Fig. 5e) whereas NSPCs in the HAMC and fiber/HAMC composites remained more evenly distributed, forming smaller spheres and interacting with the fibers as at day 2. The difference in persistence length between the coiled collagen fibers (Fig. 5c and g) and extended P(CL:DLLA) fibers (Fig. 5d and h) after sonication likely reflects the characteristics of collagen fibers to be gel-like while the P(CL:DLLA) fibers to be glassy.[24,25]

A similar cellular response was observed for cultures in differentiation media where cells in media aggregated from day 2 (Fig. 5i) to day 7 (Fig. 5m) whereas those in HAMC remained more dispersed at both day 2 (Fig. 5j) and day 7 (Fig. 5n). The NSPCs appeared to interact with both collagen (Fig. 5k and o) and P(CL:DLLA) (Fig. 5l and p) fibers at day 2 and day 7, with greater interaction apparent at 7 days. The NSPCs seemed to adhere and extend along the P(CL:DLLA) fibers most clearly (Fig. 5p) as was observed when cells were cultured in proliferation media. Thus the cellular interaction with the hydrogel/composite was dominated more by the 3D microenvironment than the media.

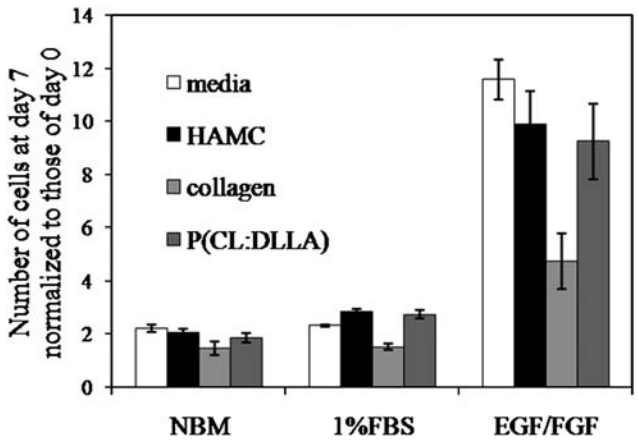

Fig. 6 NSPC viability studied over 7 days using the PicoGreen Assay for dsDNA. Cell viability was similar for all samples in each of the media conditions studied except the electrospun collagen/HAMC composite system where there were fewer viable cells in all media conditions than the other systems tested—media, HAMC and electrospun P(CL:DLLA)/HAMC composite.

Cell viability was studied over 7 days using the PicoGreen assay for dsDNA (Fig. 6). Importantly, cell viability was similar for all samples in each of the media conditions studied except the electrospun collagen/HAMC composite system where there were fewer viable cells in all media conditions than the other systems tested—media, HAMC and electrospun P(CL:DLLA)/HAMC composite. Neither collagen nor P(CL:DLLA) electrospun fibers released cytotoxic factors; thus, the decreased number of viable cells in the presence of collagen fibers suggests either a contact mediated mechanism or perhaps a high local concentration of unreacted cytotoxic genipin released.

3.6 NSPC differentiation profile in fiber/HAMC composite

The NSPC differentiation profile in the three media (NBM, 1% FBS and EGF/FGF2) and the different matrices (media, HAMC, electrospun collagen/HAMC, electrospun P(CL:DLLA)/HAMC) was assessed using quantitative RT-PCR. The expression level of the gene of interest was evaluated against the housekeeping gene, hypoxanthine phosphoribosyltransferase (HPRT) (Fig. 7). The genes selected were: nestin for progenitor cells (Fig. 7a), βIII-tubulin for neurons (Fig. 7b), CNPase for oligodendrocytes (Fig. 7c), and GFAP for astrocytes (Fig. 7d).

As shown in Fig. 7a, NSPCs grown in all media and all matrices expressed the gene for nestin, with the highest expression found for cells in the proliferation media with EGF/FGF2. This is consistent with previous results where EGF/FGF2 mitogens promote proliferation of precursor cells *vs.* differentiation. In Fig. 7b, the βIII-tubulin gene expression was similar across matrices in each media group and greatest for NSPCs cultured in NBM and 1% FBS-supplemented media. Interestingly, the greatest βIII-tubulin gene expression was found for NSPCs cultured in NBM in P(CL:DLLA)/HAMC composite gels, suggesting that these materials have a greater influence on gene expression than the media. In contrast, the NSPCs cultured in NBM and 1% FBS in collagen fiber/HAMC composite gels had the lowest βIII-tubulin gene expression, confirming the importance of the extracellular environment. The βIII-tubulin gene expression was lowest for cells cultured in EGF/FGF2, as may have been expected for the proliferation medium. A similar trend was observed for CNPase gene expression (Fig. 7c). NSPCs cultured in NMB and 1% FBS in P(CL:DLLA) fiber/HAMC composite gels had the greatest CNPase gene expression whereas those cultured in collagen fiber/HAMC composite gels had the least. Again the EGF/FGF2 medium overwhelmed the CNPase gene expression and there was no difference across groups. The GFAP gene expression was influenced primarily by the medium (and not the matrix) as shown in Fig. 7d, where the only differences observed, within one medium, were for the collagen fiber/HAMC composite system. Otherwise, the differences in GFAP gene expression were as expected, greatest in the 1% FBS differentiation medium and NBM and least in the proliferation EGF/FGF2 medium. Notwithstanding these differences in gene expression, we note that immunocytochemistry would have

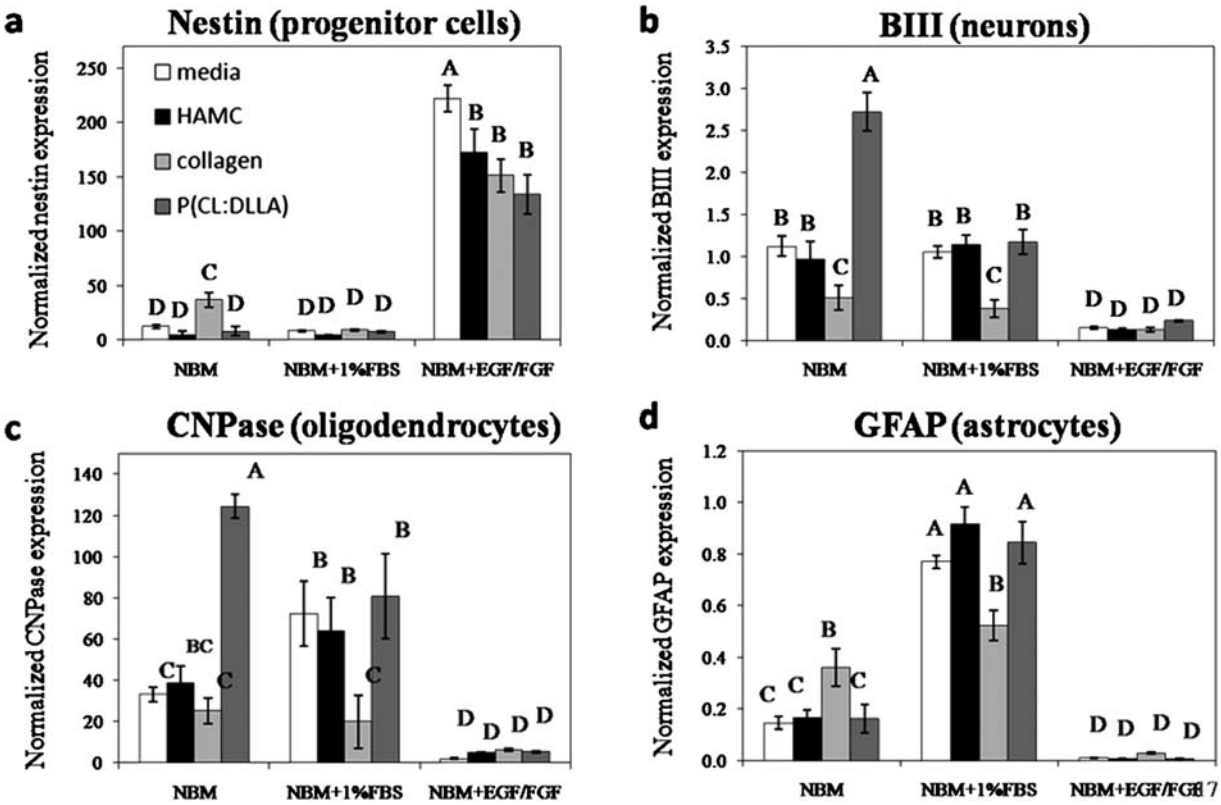

Fig. 7 The gene expression profile at day 7 for NSPCs cultured in one of three media—serum-free neural basal media (NBM), differentiation media of NBM supplemented with 1% FBS, proliferation media of NBM supplemented with EGF/FGF2—and one of four matrices: media (control), HAMC, collagen fiber/HAMC composite, P(CL:DLLA) fiber/HAMC composite. The NSPCs were studied in terms of their gene expression profiles of: (a) nestin for progenitor cells; (b) βIII-tubulin for neurons; (c) CNPase for oligodendrocytes; and (d) GFAP for astrocytes.

provided greater insight into the numbers of cells expressing the differentiation markers; however, immunocytochemistry was complicated by the 3D geometry.

4 Discussion

In order to design a scaffold for stem cell delivery to the injured spinal cord, we were constrained by ease of use and efficacy. A minimally invasive strategy results in better patient outcomes and thus an injectable, fast gelling hydrogel was pursued. While 3-dimensional by design, hydrogels often do not provide a substrate for cell adhesion, which was overcome in our system by the incorporation of electrospun fibers that were still injectable through a 30 gauge needle. While few report directly on survival, most acknowledge low rates after transplantation. We hypothesized that by controlling the microenvironment, we could achieve greater survival. To this end, we investigated low modulus hydrogels, which are known to favour differentiation of neural stem/progenitor cells to neurons and oligodendrocytes[6] and included electrospun fibers to which the NSPCs could attach. We chose two well-studied fibers—one naturally occurring collagen and one synthetic P(CL:DLLA). The latter is similar to a synthetic PCL electrospun fiber that had been previously shown to promote differentiation to oligodendrocytes.[26] With the view of testing this cell delivery vehicle *in vivo*, we mimicked the *in vivo* injection strategy by testing our cell-composite hydrogel strategies after injection from a 30 gauge needle.

Importantly, the hyaluronan/methylcellulose (HAMC) hydrogel forms a gel at 37 °C in the presence of NSPCs and is easily injected through a 30 gauge syringe because it is a shear thinning fluid at lower temperatures.[27] Since the cells are easily dispersed in HAMC and their distribution maintained over several days of culture, cell damage during processing is limited and heterogeneous distribution avoided, unlike some other cell seeding techniques.[28] In the media alone controls, NSPCs aggregated to form neurospheres which, at a certain size, limit the diffusion of nutrients and oxygen to the core, resulting in necrotic centers.[29,30] In contrast, HAMC maintained an even dispersion of NSPCs in 3D and minimized cell sedimentation and aggregation. The importance of HAMC to cell distribution was most profound in the proliferation media where cell density increased substantially over time, forming large cell aggregates in media and some cell death, but not in HAMC. The ease of cell seeding and distribution is important to eventual host tissue survival and integration.[31] The use of HAMC may also provide a uniform environment to all transplanted cells, avoiding some of the heterogeneous behaviour observed from cells at the core *vs.* those at the periphery of the implant.[32] Moreover, since we envision injecting the cells into tissue, it was significant that HAMC swelled only minimally, thereby reducing the risk of secondary compression at the injury site.

By studying cell behaviour in different media and hydrogel microenvironments, we found that the metabolic activity of the cells depended on whether the cells were proliferating or differentiating. Here, we report, for the first time, that NSPCs have higher total plasma ATP content when proliferating, as supported by data in Fig. 3b where the majority of cells are proliferating. Interestingly, this finding is somewhat controversial since Cho *et al.* and Lonergan *et al.* reported an increase of ATP content in human embryonic stem cells and stromal stem cells, respectively, when cells differentiate.[33,34] On the other hand, Park *et al.* found higher mitochondria metabolic activity when human corneal endothelial cells proliferate.[35] Clearly, metabolic activity is a function of cell type and cell state, making comparisons across different cell types and culture conditions difficult.

The polymeric microenvironment acts as a template for cell adhesion, survival and differentiation.[36] Electrospun fibers were incorporated into HAMC to promote cell–matrix interactions. Collagen scaffolds have been shown to facilitate neural stem/progenitor cell transplantation and to promote recovery in the injured spinal cord[37] while biodegradable synthetic P(CL:DLLA) have been widely used as tissue-engineering scaffolds and shown to be biocompatible to NSPC.[38] Unexpectedly, the electrospun collagen fibers were deleterious to NSPC survival/proliferation and differentiation profiles whereas P(CL:DLLA) sustained NSPC viability and guided cellular differentiation to neurons and oligodendrocytes, similar to HAMC. It has been shown in literature that nanotopographical features including fiber diameter, surface morphology, as well as mechanical strength can alter cell behaviour.[39–41] Hence, the inability of collagen fibers to support differentiation of NSPCs may be due more to their fine, fragmented, and tangled structures *vs.* the chemical composition, especially since the P(CL:DLLA) fibers modulated NSPC differentiation towards desirable oligodendrocytes without the addition of growth factors. Of course, exogenous factors impact the differentiation profile. In media containing 1% FBS, CNPase and GFAP gene expression were higher relative to basic media which is similar to what has been observed by others.[42,43]

5 Conclusions

Overall, we found that the cellular microenvironment is defined by the media and the hydrogel composite and each of these can influence the differentiation and proliferation profiles of NSPCs. The HAMC 0.5/0.5 w/w% provided a facile hydrogel for stable cell distribution and delivery through an injectable delivery strategy. The inclusion of electrospun fibers in the hydrogel composite promoted cell survival and guided cell differentiation similar to HAMC alone, yet different from media controls, demonstrating the importance of 3D culture to cell behaviour. Of the two electrospun fibers examined, the P(CL:DLLA)/HAMC composite was most suitable for NSPC survival and differentiation towards neuronal and oligodendrocytic phenotypes. Oligodendrocytes are compelling in regenerative strategies of the spinal cord as they produce myelin which limits axonal degeneration and promotes proper functioning of regenerated axons. Future studies will evaluate these systems *in vivo* for NSPC survival and differentiation in established rodent SCI models.

Acknowledgements

We thank Ying Fang Chen for her assistance with the cell culture. We are grateful to the Advanced Food and Materials Network for funding this collaborative research (MSS, BA, WW), to NSERC for a graduate student scholarship (AH) and to the McEwen Center in Regenerative Medicine for a post-doctoral fellowship (YL).

References

1 C. E. Hulsebosch, Recent advances in pathophysiology and treatment of spinal cord injury, *Adv. Physiol. Educ.*, 2002, **26**, 238–255.
2 G. Martino and S. Pluchino, The therapeutic potential of neural stem cells, *Nat. Rev. Neurosci.*, 2006, **7**, 395–406.
3 S. Karimi-Abdolrezaee, E. Eftekharpour, J. Wang, C. M. Morshead and M. G. Fehlings, Delayed transplantation of adult neural precursor cells promotes remyelination and functional neurological recovery after spinal cord injury, *J. Neurosci.*, 2006, **26**, 3377–3389.
4 A. M. Parr, I. Kulbatski and C. H. Tator, Transplantation of adult rat spinal cord stem/progenitor cells for spinal cord injury, *J. Neurotrauma*, 2007, **24**, 835–845.
5 B. J. Cummings, N. Uchida, S. J. Tamaki, D. L. Salazar, M. Hooshmand, R. Summers, F. H. Gage and A. J. Anderson, Human neural stem cells differentiate and promote locomotor recovery in spinal cord-injured mice, *Proc. Natl. Acad. Sci. U. S. A.*, 2005, **102**, 14069–14074.
6 N. D. Leipzig and M. S. Shoichet, The effect of substrate stiffness on adult neural stem cell behavior, *Biomaterials*, 2009, **30**, 6867–6878.
7 F. Cao, A. H. S. Rafie, O. J. Abilez, H. Wang, J. T. Blundo, B. Pruitt, C. Zarins and J. C. Wu, *In vivo* imaging and evaluation of different biomaterials for improvement of stem cell survival, *J. Tissue Eng. Regener. Med.*, 2007, **1**, 465–468.
8 G. A. Silva, C. Czeisler, K. L. Niece, E. Beniash, D. A. Harrington, J. A. Kessler and S. I. Stupp, Selective differentiation of neural progenitor cells by high-epitope density nanofibers, *Science*, 2004, **303**, 1352–1355.
9 Y. Luo and M. S. Shoichet, A photolabile hydrogel for guided three-dimensional cell growth and migration, *Nat. Mater.*, 2004, **3**, 249–253.
10 N. D. Leipzig, C. Xu, T. Zahir and M. S. Shoichet, Functional immobilization of interferon-gamma reduces neuronal differentiation of neural stem cells, *J. Biomed. Mater. Res., Part A*, 2009, **93A**, 625–633.
11 D. D. Allison, Review. Hyaluronan: a powerful tissue engineering tool, *Tissue Eng.*, 2006, **12**, 2131–2140.
12 D. Gupta, C. H. Tator and M. S. Shoichet, Fast-gelling injectable blend of hyaluronan and methylcellulose for intrathecal, localized delivery to the injured spinal cord, *Biomaterials*, 2006, **27**, 2370–2379.
13 N. Sarkar, Thermal gelation properties of methyl and hydroxypropyl methylcellulose, *J. Appl. Polym. Sci.*, 1979, **24**, 1073–1087.
14 M. C. Tate, D. A. Shear, S. W. Hoffman, D. G. Stein and M. C. LaPlaca, Biocompatibility of methylcellulose-based constructs designed for intracerebral gelation following experimental traumatic brain injury, *Biomaterials*, 2001, **22**, 1113–1123.
15 F. Z. Cui, W. M. Tian, S. P. Hou, Q. Y. Xu and I.-S. Lee, Hyaluronic acid hydrogel immobilized with RGD peptides for brain tissue engineering, *J. Mater. Sci.*, 2006, **17**, 1393–1401.
16 W. M. Tian, S. P. Hou, J. Ma, C. L. Zhang, Q. Y. Xu, I. S. Lee, H. D. Li, M. Spector and F. Z. Cui, Hyaluronic acid-poly-D-lysine-based three dimensional hydrogel for traumatic brain injury, *Tissue Eng.*, 2005, **11**, 513–525.
17 W. Wan and M. Mekhail, Compositions and methods to cross link polymer fibers, *US Pat.*, 61/117997, 2009.
18 M. Mekhail, K. K. H. Wong, Y. Wu, D. B. O'Gorman and W. Wan, Genipin-crosslinked electrospun collagen fibers, *Biomacromolecules*, 2010, submitted.
19 J. W. S. Hayami, D. C. Surrao, S. D. Waldman and B. G. Amsden, Design and characterizationof a biodegradable composite scaffold for ligament tissue engineering, *J. Biomed. Mater. Res., Part A*, 2009, **92**, 1407–1420.
20 T. Zahir, H. Nomura, X. D. Guo, H. Kim, C. Tator, C. Morshead and M. Shoichet, Bioengineering neural stem/progenitor cell-coated

tubes for spinal cord injury repair, *Cell Transplant.*, 2008, **17**, 245–254.
21 N. D Leipzig and M. S. Shoichet, The effect of substrate stiffness on adult neural stem cell behavior, *Biomaterials*, 2009, **30**, 6867–6878.
22 T.-T. Hsieh, C. Tiu and G. P. Simon, Rheological behaviour of polymer blends containing only hyperbranched polyesters of varying generation number, *Polymer*, 2001, **42**, 7635–7638.
23 T. Zahir, Y. F. Chen, J. F. MacDonald, N. Leipzig, C. H. Tator and M. S. Shoichet, Neural stem/progenitor cells differentiate *in vitro* to neurons by the combined action of dibutyryl camp and interferon-gamma, *Stem Cells Dev.*, 2009, **18**(10), 1423–1432.
24 Z.-P. Luo, Y.-L. Sun, T. Fujii and K.-N. An, Single molecule mechanical properties of type II collagen and hyaluronan measured by optical tweezers, *Biorheology*, 2004, **41**, 247–254.
25 M. Crne, J. O. Park and M. Srinivasarao, Electrospinning physical gels: the case of stereocomplex PMMA, *Macromolecules*, 2009, **42**, 4353–4355.
26 D. R. Nisbet, L. M. Yu, T. Zahir, J. S. Forsythe and M. S. Shoichet, Characterization of neural stem cells on electrospun poly (ε-caprolactone) submicron scaffolds: evaluating their potential in neural tissue engineering, *J. Biomater. Sci., Polym. Ed.*, 2008, **19**, 623–634.
27 C. E. Kang, P. C. Poon, C. H. Tator and M. S. Shoichet, A new paradigm for local and sustained release of therapeutic molecules to the injured spinal cord for neuroprotection and tissue repair, *Tissue Eng. A*, 2009, **15**, 595–604.
28 L. A. Solchaga, E. Tognana, K. Penick, H. Baskaran, V. M. Goldberg, A. I. Caplan and J. F. Welter, A rapid seeding technique for the assembly of large cell/scaffold composite constructs, *Tissue Eng.*, 2006, **12**, 1851–1863.
29 D. R. Wakeman, M. R. Hofmann, Y. D. Teng and E. Y. Snyder, Neural progenitors, *Hum. Cell Cult.*, 2009, **7**, 1–44.
30 A. Bez, E. Corsini, D. Curti, M. Biggiogera, A. Colombo, R. F. Nicosia, S. F. Pagano and E. A. Parati, Neurosphere and neurosphere-forming cells: Morphological and ultrastructural characterization, *Brain Res.*, 2003, **993**, 18–29.
31 B. G. Ballios, M. J. Cooke, D. van der Kooy and M. S. Shoichet, A hydrogel-based stem cell delivery system to treat retinal degenerative diseases, *Biomaterials*, 2010, **31**, 2555–2564.
32 E. Bible, D. Y. S. Chau, M. R. Alexander, J. Price, K. M. Shakesheff and M. Modo, The support of neural stem cells transplanted into stroke-induced brain cavities by PLGA particles, *Biomaterials*, 2009, **30**, 2985–2994.
33 Y. M. Cho, S. Kwon, Y. K. Pak, H. W. Seol, Y. M. Choi, D. J. Park, K. S. Park and H. K. Lee, Dynamic changes in mitochondrial biogenesis and antioxidant enzyme during the spontaneous differentiation of human embryonic stem cells, *Biochem. Biophys. Res. Commun.*, 2006, **348**, 1472–1478.
34 T. Lonergan, C. Brenner and B. Bavister, Differentiation-related changes in mitochondrial properties as indicators of stem cell competence, *J. Cell. Physiol.*, 2006, **208**, 149–153.
35 C. Y. Park, Z. Zhu, C. Zhang, C. S. Moon and R. S. Chunk, Cellular redox state predicts *in vitro* corneal endothelial cell proliferation capacity, *Exp. Eye Res.*, 2006, **83**, 903–310.
36 A. I. Teixeira, J. K. Duckworth and O. Hermanson, Getting the right stuff: controlling neural stem cell state and fate *in vivo* and *in vitro* with biomaterials, *Cell Res.*, 2007, **17**, 56–61.
37 M. Hatami, N. Z. Mehrjardi, S. Kiani, K. Hemmesi, H. Azizi, A. Shahverdi and H. Baharvand, Human embryonic stem-derived neural precursor transplants in collagen scaffolds promote recovery in injured rat spinal cord, *Cytotherapy*, 2009, 1–13.
38 S. H. Bhang, J. S. Lim, C. Y. Choi, Y. K. Kwon and B.-S. Kim, The behavior of neural stem cells on biodegradable synthetic polymers, *J. Biomater. Sci., Polym. Ed.*, 2007, **18**, 223–239.
39 G. T. Christopherson, H. Song and H.-Q. Mao, The influence of fiber diameter of electrospun substrates on neural stem cell differentiation and proliferation, *Biomaterials*, 2009, **30**, 556–564.
40 J. M. Corey, C. C. Gertz, B.-S. Wang, L. K. Birrell, S. L. Johnson, D. C. Martin and E. L. Feldman, The design of electrospun PLLA nanofiber scaffolds compatible with serum-free growth of primary motor and sensory neurons, *Acta Biomater.*, 2008, **4**, 863–875.
41 I. K. Kwon, K. Satoru and M. Takehisa, Electrospun nano to microfiber fabrics made of biodegradable copolyesters: structural characteristics, mechanical properties and cell adhesion potential, *Biomaterials*, 2005, **26**, 3929–3939.
42 M. Jana, A. Jana, U. Pal and K. Pahan, A simplified method for isolating highly purified neurons, oligodendrocytes, astrocytes, and microglia from the same human fetal brain tissue, *Neurochem. Res.*, 2007, **32**, 2015–2022.
43 J. E. Bottenstein, Growth requirements *in vitro* of oligodendrocyte cell lines and neonatal rat brain oligodendrocytes, *Proc. Natl. Acad. Sci. U. S. A.*, 1986, **83**, 1955–1959.